



Antibacterial activity of nanostructured Ti–45S5 bioglass–Ag composite against *Streptococcus mutans* and *Staphylococcus aureus*

K. JURCZYK¹, M. M. KUBICKA², M. RATAJCZAK², M. U. JURCZYK³, K. NIESPODZIANA⁴,
D. M. NOWAK², M. GAJECKA^{2,5}, M. JURCZYK⁴

1. Department of Conservative Dentistry and Periodontology, Poznan University of Medical Sciences,
Bukowska 70, Poznan 60-812, Poland;

2. Faculty of Pharmacy, Department of Genetics and Pharmaceutical Microbiology,
Poznan University of Medical Sciences, Swiecickiego 4, Poznan 60-781, Poland;

3. Division of Mother's and Child's Health, Poznan University of Medical Sciences, Polna 33, Poznan 60-535, Poland;

4. Institute of Materials Science and Engineering, Poznan University of Technology,
Jana Pawla II 24, Poznan 61-138, Poland;

5. Institute of Human Genetics, Polish Academy of Sciences, Strzeszynska 32, Poznan 60-479, Poland

Received 3 February 2015; accepted 20 August 2015

Abstract: Mechanical alloying and annealing at 1150 °C for 2 h under an argon atmosphere were used to prepare Ti–45S5 bioglass nanocomposites. Ti–45S5 bioglass material was chemically modified by silver. The antibacterial activity of Ti–10% 45S5 bioglass nanocomposite containing silver against *Streptococcus mutans* and *Staphylococcus aureus* was studied. Nanocomposites were characterized by X-ray diffraction, scanning electron microscopy equipped with an electron energy dispersive spectrometer and transmission electron microscopy to evaluate phase composition, crystal structure and grain size. *In vitro* bacterial adhesion study indicated a significantly reduced number of *Streptococcus mutans* and *Staphylococcus aureus* on the bulk nanostructured Ti–45S5 bioglass–Ag plate surface in comparison to that on microcrystalline Ti plate surface. Nanostructured Ti-based biomaterials can be considered to be the future generation of dental implants.

Key words: 45S5 bioglass; antimicrobial activity; silver; titanium; dental implant; *Streptococcus mutans*; *Staphylococcus aureus*

1 Introduction

Nanostructured materials have the potential to be used in dentistry for infection control and the management of the oral biofilm [1]. These nanomaterials include solid nanoparticles of metal or metal oxides, and nanocomposites [2,3]. Titanium and its alloys are preferred materials in the production of medical implants [2,4–6]. Much attention is paid to enhance the strength characteristics of Ti-based alloys in order to avoid potential biotoxicity of alloying elements [7,8].

Improvement of the physicochemical and mechanical performance of Ti-based implant materials can be achieved by microstructure control [1,2,6,9–11]. Recent studies have shown clearly that titanium nanostructures considerably improve both the mechanical properties and the biocompatibility [2].

The nanocomposite materials containing titanium and bioceramic (hydroxyapatite (HA, $\text{Ca}_{10}(\text{PO}_4)_6(\text{OH})_2$), 45S5 bioglass or silica (SiO_2) as a reinforced phase are promising alternatives to conventional microcrystalline materials [10,11–15]. For example, Ti-based nanocomposites reinforced with 10%–20% 45S5 bioglass particles were fabricated by the mechanical alloying (MA) and powder metallurgy technique [14].

Our results of *in vitro* studies showed that these bionanocomposites had excellent biocompatibility and could integrate with bone. Furthermore, the addition of 45S5 bioglass to titanium has a positive effect on the corrosion resistance of titanium in Ringer's solution [14]. The Vickers microhardness for Ti–10% 45S5 bioglass nanocomposites reaches $\text{HV}_{0.2}$ 620, which is higher than that of pure microcrystalline Ti metal ($\text{HV}_{0.2}$ 225). This effect is directly connected with structure refinement and obtaining of nanostructure. Additionally, the

nanostructured Ti–10% 45S5 bioglass composites possess higher fracture toughness ($K_{IC}=1.75 \text{ MPa}\cdot\text{m}^{1/2}$) compared with 45S5 bioglass ($K_{IC}=0.6 \text{ MPa}\cdot\text{m}^{1/2}$) [16].

Moreover, the structure, corrosion and biological properties of porous titanium–45S5 bioglass nanocomposite scaffolds were studied [17,18]. The materials have low density and a structure composed of an interconnected network of pores. The porous Ti–10% 45S5 bioglass nanocomposite scaffolds have porous architecture, with macropores of 400–800 μm and micropores of some tens of micrometers. The results of the *in vitro* biocompatibility test suggest that Ti–10%45S5 bioglass nanocomposite scaffolds display better biocompatibility compared with microcrystalline titanium and the normal human osteoblast (NHOst) cells grew on the surface and inside the pores and showed good spreading.

The antibacterial properties of silver have been exploited in medicine for infection control [19]. Silver particles showed strong bactericidal potential against both Gram-positive and Gram-negative bacteria. Recently, the vacuum plasma spraying technique has been successfully used to apply silver-containing HA coating material to a titanium alloy generating a compound material with antibacterial properties [20]. *In vitro* bacterial biofilm inhibition study indicated a significantly inhibited biofilms formation of *S. aureus* and *P. aeruginosa* strains on HA/Ag coating compared with HA coating alone. The Ag^+ partially substitutes calcium and enters the structure of hydroxyapatite [21].

The aim of this study was to assess the antibacterial activity of Ti–10% 45S5 bioglass nanocomposite containing silver against *Streptococcus mutans* and *Staphylococcus aureus*. Silver particles may release ions by dissolution. Yet, to the authors knowledge, there are no published articles regarding the *in vitro* antibacterial properties of nanostructured Ti-based composites with 45S5 bioglass against *S. mutans*. *S. mutans* is frequently identified within the oral cavity and is associated with dental caries, oral infections and periodontal disease. On the other hand, *S. aureus* has long been recognized as one of the most important bacteria that cause diseases in humans and serious infections such as bloodstream infections, pneumonia, bone and joint infections. Conducted research evaluated the influence of chemical composition of Ti-based nanocomposite on the biofilm formation. Based on our previous results, 10% 45S5 bioglass in titanium is the best choice for further investigation [14].

2 Experimental

2.1 Sample preparation

The present work contains results of research

carried out for bulk Ti–10% 45S5 bioglass and Ti–10% 45S5 bioglass–1.5% Ag nanocomposites. For purpose of brevity, in this study, materials are denoted as follows: Ti–10% 45S5 bioglass is labeled as Ti–45S5 bioglass and Ti–10% 45S5 bioglass–1.5% Ag is labeled as Ti–45S5 bioglass–Ag.

The starting materials used were titanium (<45 μm , 99.5%, Alfa Aesar), 45S5 bioglass (44.8% SiO_2 , 24.9% Na_2O , 24.5% CaO , 5.8% P_2O_5 with powder size of 53 μm , MO-SCI Health Care LLC) and silver (4–7 μm , 99.9%, Alfa Aesar). Elemental powders were weighed, blended and poured into vials in glove box (Labmaster 130) filled with automatically controlled argon atmosphere ($\text{O}_2 \leq 2 \times 10^{-6}$ and $\text{H}_2\text{O} \leq 1 \times 10^{-6}$). MA was performed under argon atmosphere using SPEX 8000 Mixer Mill. After 15 h of MA, the amorphous powders were uniaxially pressed (8 mm in diameter and 3 mm in height) at a compacting pressure of 800 MPa. Finally, the green compacts were heat-treated at 1150 $^\circ\text{C}$ for 2 h under an argon atmosphere (99.999% purity) to form ordered phases. The discs of the synthesized samples as well as microcrystalline Ti (grade 2) polished with 1200 SiC paper in water and ultrasonically rinsed with acetone were used for all tests.

2.2 Material characterization

The phase constitution of Ti-based nanocomposites was analyzed by X-ray diffraction with Cu $K_{\alpha 1}$ radiation. The crystallite sizes (L) were estimated by the Scherrer method according to the following equation:

$$B(2\theta) = \frac{K\lambda}{L \cos \theta} \quad (1)$$

where peak width B is inversely proportional to crystallite size L , K is a dimensionless shape factor with a value close to unity. The shape factor has a typical value of about 0.9, but varies with the actual shape of the crystallite. λ is the X-ray wavelength; B is the line broadening at half the maximum intensity (FWHM); after subtracting the instrumental line broadening, in radians; and θ is the Bragg angle.

Scanning electron microscope (SEM) with energy dispersive spectrometer (EDS) was used to characterize the microstructure and chemical composition of the prepared samples. The TEM images and selected area electron diffraction (SAED) patterns were recorded with a Philips CM 20 Super Twin microscope, which provides 0.24 nm resolution at an acceleration voltage of 200 kV.

2.3 Assessment of biofilm formation inhibition

2.3.1 *Streptococcus mutans*

The strain of *S. mutans*, obtained from the American Type Culture Collection (ATCC 27351), was assessed in this study. Liquid bacterium culture in 5 mL of Tryptic

Soy Broth (TSB) was incubated overnight at $(36\pm 1)^\circ\text{C}$. The resulting log phase culture had a concentration of $\sim 10^8$ CFU/mL (colony-forming unit/mL). The experimental samples were placed in three 12-well plates followed by the addition of 4.5 mL TSB and 0.5 mL of the bacterial suspension. Titrated plates were incubated at $(36\pm 1)^\circ\text{C}$ with shaking at 200 r/min, for 4 h or 20 h.

Two methods, qualitative SEM and quantitative dilution method were used to assess bacterium adherence to different experimental material surfaces. In the two qualitative assessments of three plates, one after 4 h and the second after 20 h of incubation, were gently rinsed three times with phosphate buffered saline (PBS) in order to eliminate the non-adherent bacterium cells and prepared before SEM. The research material was fixated in 2.5% glutaraldehyde in phosphate buffer. Then, it was dehydrated at a temperature of 50°C in a concentration range of ethanol from 25% to 100%. After disc drying, the samples were sprayed with gold in a sputter ionization process. At the end of the experiment, samples in a SEM were observed and then images were taken. In the quantitative assessment, the third plate, at the end of the 20 h incubation period was gently rinsed three times with PBS in order to eliminate the non-adherent bacteria. Then, the samples were put into individually new plates containing 5 mL PBS each, and samples were vortexed for 60 s to release the adherent microorganisms. The viable cells in the buffer were quantified by serial dilutions on Columbia agar with 5% blood plates. Columbia agar plates were incubated at $(36\pm 1)^\circ\text{C}$, and the CFU was counted. The quantitative experiments were repeated three times. The statistical significance was defined as $p < 0.05$.

2.3.2 *Staphylococcus aureus*

Cultures of *S. aureus* (ATCC 6538) were obtained from commercial sources (American Type Culture Collection), and an aliquot was inoculated into 5 mL TSB overnight. The resulting log-culture had a concentration of $\sim 10^9$ CFU/mL. The experimental samples were placed in 5 mL sterilized tubes followed by the addition of 0.5 mL bacterial suspension to TSB. The tubes were incubated at 37°C with shaking at 200 r/min for 3 h. At the end of the incubation period, the samples were gently rinsed three times with PBS in order to eliminate the non-adherent bacteria. Then, the samples were put into individually new tubes containing 5 mL PBS each, and then subjected to sonication at a frequency of 20 kHz (Bandelin Sonoplus) for 5 min, followed by additional vortexing for 60 s to remove the adhering micro-organisms. The viable organisms in the buffer were quantified by plating serial dilutions on Tryptic Soy agar (TSA) plates. TSA plates were incubated at 37°C , and the colony-forming units were counted visually. Additionally, qualitative SEM was used to

assess bacterium adhered to different experimental material surfaces.

3 Results

In the present work, bulk Ti–45S5 bioglass and Ti–45S5 bioglass–Ag nanocomposites were produced by MA and powder metallurgy process. The influence of microstructure and chemical composition of Ti-based nanocomposite on the biofilm formation was evaluated.

3.1 Structure properties

Ti–45S5 bioglass and Ti–45S5 bioglass–Ag nanocomposites were synthesized. Figures 1(a)–(c) show the XRD patterns of the starting microcrystalline titanium (ICDD: 5–682), amorphous 45S5 bioglass and Ag (ICDD: 4–783) powders. During MA process, the titanium, 45S5 bioglass and Ag particles are periodically trapped between colliding balls and are plastically deformed. The intensity of diffraction lines of titanium decreases with milling time (not shown), and after 15 h of milling, titanium transforms to an amorphous phase with trace content of nanocrystalline Ti (101) (Fig. 1(d)). According to the Scherrer method of XRD profile, the mean crystallite size of this nanocrystal is about 9 nm.

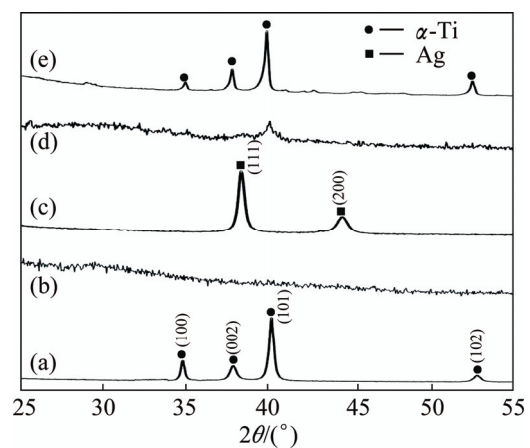


Fig. 1 XRD patterns of Ti, 45S5 bioglass and silver powders mechanically alloyed for different time: (a) Ti, 0 h; (b) 45S5 bioglass, 0 h; (c) Ag, 0 h; (d) 15 h of MA; (e) Bulk Ti–45S5 bioglass–Ag nanocomposite after annealing at 1150°C for 2 h

The formation of the bulk Ti–45S5 bioglass and Ti–45S5 bioglass–Ag nanocomposites was achieved by annealing of the amorphous materials in high purity argon atmosphere at 1150°C for 2 h. SEM image of the Ti–45S5 bioglass–Ag nanocomposite with porosity of 8% is shown in Fig. 2. The sample exhibited wide cavities, 3–9 μm in diameter. XRD analysis of Ti–bioglass–Ag showed the presence of α -Ti type structure with cell parameters $a=2.963 \text{ \AA}$, $c=4.756 \text{ \AA}$ (Fig. 1(e)). When silver is added to Ti–10% 45S5

bioglass, the lattice constants of Ti–45S5 bioglass composite decrease (Table 1). Silver has lower atomic diameter in comparison with titanium. The thermal treatment of 45S5 bioglass at 800 °C results in the development of calcium phosphate crystals with a structure similar to hydroxyapatite [22]. Additionally, formation of $\text{Na}_2\text{Ca}_2\text{Si}_3\text{O}_9$ (ICDD:22–1455) as the main phase and $\text{Na}_2\text{CaSi}_3\text{O}_8$ (55S4.1) as the secondary minor phase was observed at above 600 °C [23,24].

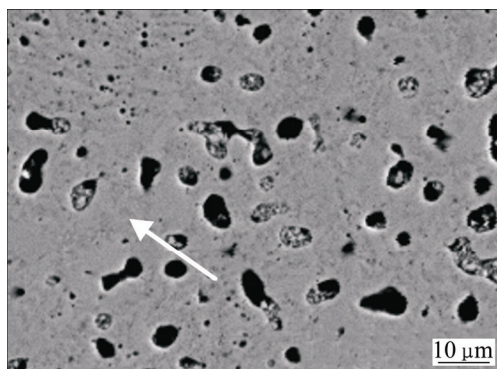


Fig. 2 SEM image of studied Ti–45S5 bioglass–Ag nanocomposite

Table 1 Structural parameters and grain sizes of studied bulk Ti–45S5 bioglass and Ti–45S5 bioglass–Ag nanocomposites in comparison to microcrystalline titanium

Sample	$a/\text{Å}$	$c/\text{Å}$	$V/\text{Å}^3$	$d/\mu\text{m}$
Ti–45S5 bioglass	2.970	4.759	36.35	0.013
Ti–45S5 bioglass–Ag	2.963	4.756	36.16	0.009
Ti (microcrystalline, grade 2)	2.948	4.784	36.01	45

The results of EDS analysis of the surface of sintered Ti–45S5 bioglass–Ag nanocomposite are shown in Fig. 3. It can be confirmed that synthesized composite mainly consists of titanium matrix with elements of Ag, O, Si, Ca, Na and P. Microstructure and possible local ordering in the Ti–45S5 bioglass–Ag samples were studied by TEM. The sample milled for 15 h was mostly amorphous as appeared from a high resolution image (Fig. 4(a)). SAED pattern (see inset in Fig. 4(a)) contains broad rings at positions expected for Ti with hexagonal structure. There are, however, additional weak, diffuse rings, most probably from TiO_2 . It has been found that the amorphous alloy was unstable upon exposure to electron beam and underwent some crystallization. Microstructure of sample annealed at 1150 °C for 2 h is shown in Fig. 4(b). Analysis of high resolution image revealed the presence of well developed crystallites with broad range of sizes from 4 nm up to more than 30 nm. SAED pattern obtained from large area (200 μm) (see inset in Fig. 4(b)) contains sharp rings corresponding to Ti.

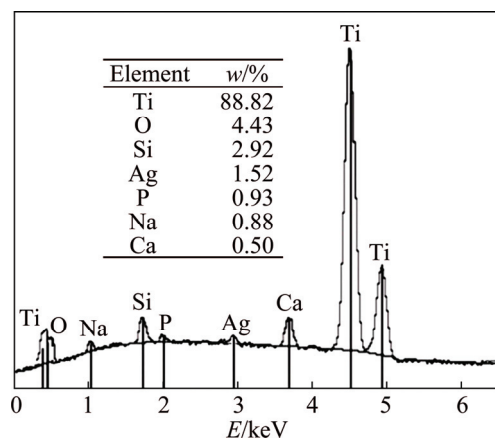


Fig. 3 EDS pattern of bulk Ti–45S5 bioglass–Ag nanocomposite (analyzed point is indicated in corresponding SEM image (Fig. 2))

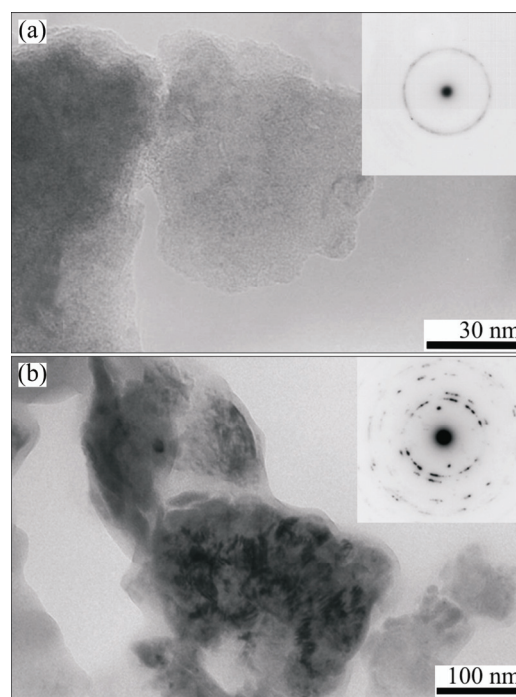


Fig. 4 TEM images and electron diffraction patterns of MA Ti–45S5 bioglass–Ag sample milled for 15 h (a) and annealed at 1150 °C for 2 h (b)

3.2 Assessment of biofilm formation inhibition

3.2.1 Qualitative assessment

The results of SEM qualitative assessment of tested microcrystalline Ti and two bulk Ti–45S5 bioglass, Ti–45S5 bioglass–Ag nanocomposites are presented in Figs. 5 and 6. These figures show evolution of inhibition of biofilm formation after 20 h of incubation. In the early stage of the biofilm formation (4 h), microcolonies of *S. mutans* and *S. aureus* were in contact one to each other in the secreted extracellular polymeric substance (EPS), irreversibly attached to the tested Ti-based nanocomposites (not shown).

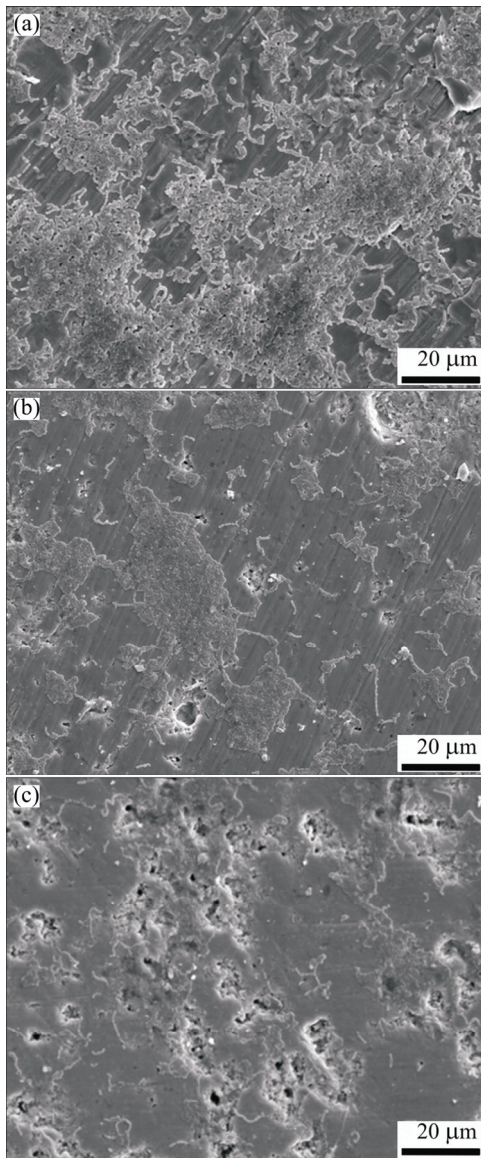


Fig. 5 SEM images showing inhibition of biofilm formation (*S. mutans*) after 20 h: (a) Microcrystalline titanium; (b) Bulk Ti-45S5 bioglass; (c) Bulk Ti-45S5 bioglass-Ag

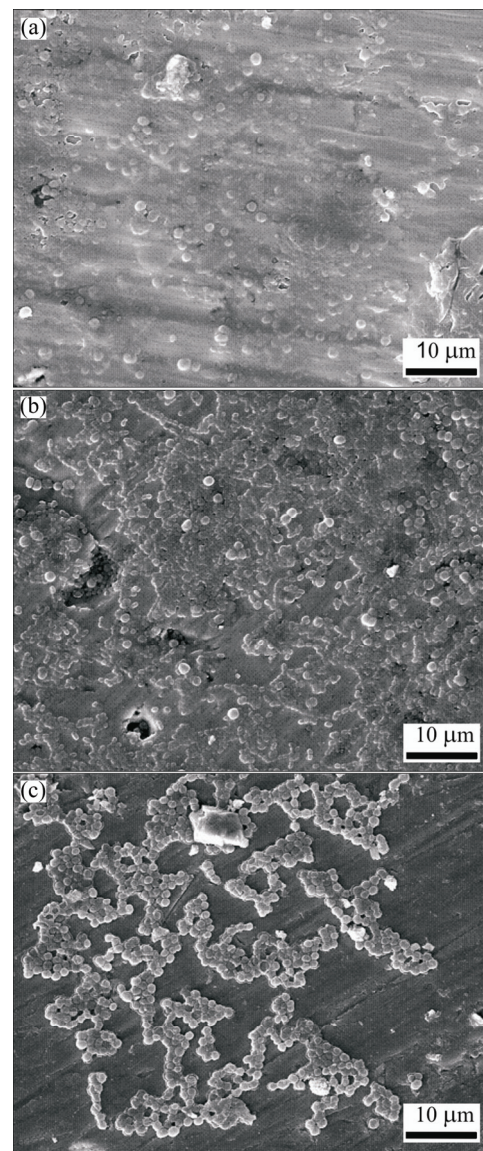


Fig. 6 SEM images showing inhibition of biofilm formation (*S. aureus*) after 20 h: (a) Microcrystalline titanium; (b) Bulk Ti-45S5 bioglass; (c) Bulk Ti-45S5 bioglass-Ag

Figures 7 and 8 show the results of viable bacteria adhered to the different experimental material surfaces when exposed to *S. mutans* and *S. aureus*. Bacterial adhesion was significantly reduced on the surface of Ti-45S5 bioglass-Ag nanocomposite when compared with the microcrystalline titanium. The Ti-45S5 bioglass-Ag nanocomposites were observed to have significantly lower adhesion of *S. mutans* and *S. aureus*, suggesting that the Ti-45S5 bioglass-Ag nanocomposites were antibacterial. It is important to note that the Ti-45S5 bioglass composite cannot exhibit antibacterial activity against *S. aureus*.

3.2.2 *In vitro* antibacterial test

Figure 9 shows the results of viable cells of *S. mutans* and *S. aureus* adhered to different experimental Ti-based nanocomposite surfaces. Bacterial biofilm

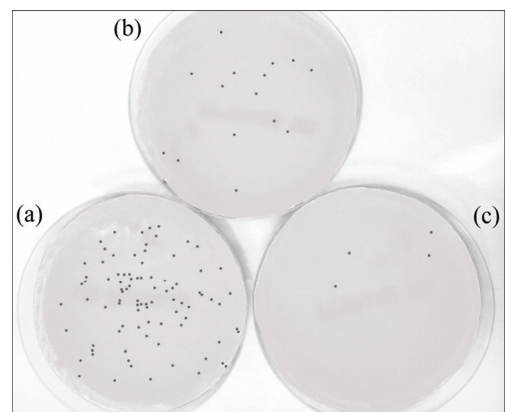


Fig. 7 Representative macroscopic photos of viable adherent *S. mutans* on different experimental material surfaces: (a) Microcrystalline titanium; (b) Bulk Ti-45S5 bioglass nanocomposite; (c) Bulk Ti-45S5 bioglass-Ag nanocomposite

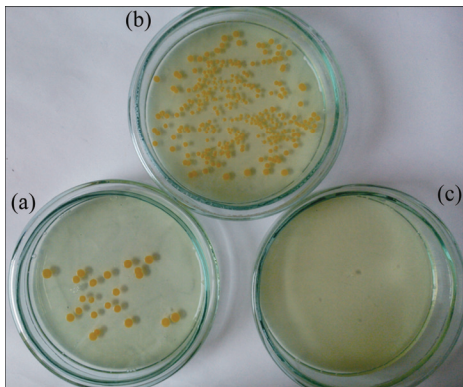


Fig. 8 Representative macroscopic photos of viable adherent *S. aureus* on different experimental material surfaces: (a) Microcrystalline titanium; (b) Bulk Ti-45S5 bioglass nanocomposite; (c) Bulk Ti-45S5 bioglass-Ag nanocomposite

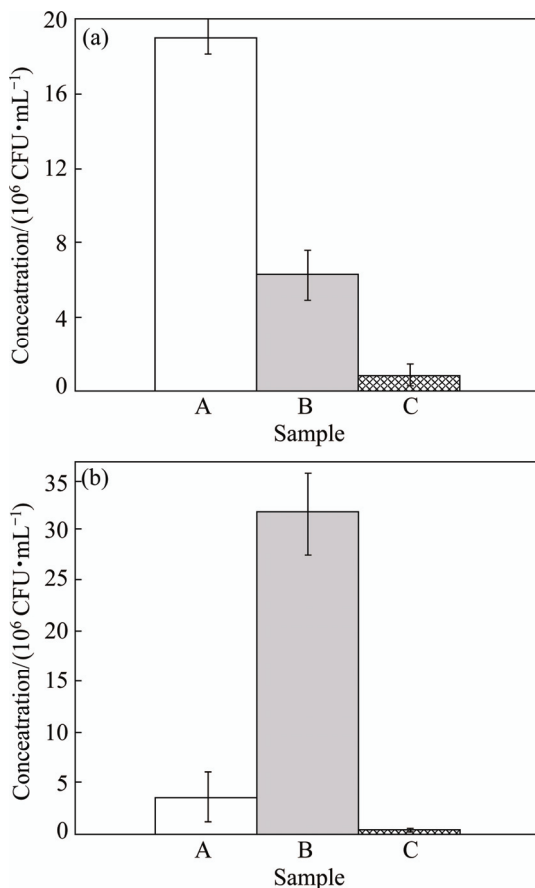


Fig. 9 Statistical results of viable adherent *S. mutans* (a) and *S. aureus* (b) on different experimental material surfaces (A—Microcrystalline titanium; B—Bulk Ti-45S5 bioglass nanocomposite; C—Bulk Ti-45S5 bioglass-Ag nanocomposite)

adhesion was significantly reduced on bulk Ti-45S5 bioglass-Ag nanocomposite when compared with control microcrystalline Ti sample. The Ti-45S5 bioglass-Ag nanocomposite was observed to have significantly lower adhesion level ($P < 0.05$) of *S. mutans* and *S. aureus*, suggesting that this bionanocomposite has inhibited biofilm formation.

4 Discussion

Nanostructuring of titanium and Ti alloys opens new possibilities for improving the long-term performance of dental implants [9,25]. Nanocrystalline metals due to extremely small grain sizes enhance physico-chemical, mechanical and biological properties compared with the corresponding materials with microcrystalline grain size. In the MA powders high plastic deformation is generated, resulting in high density of dislocation lines and subsequently subgrain formation, which finally lead to amorphisation [26]. The milled powder is then heat-treated to obtain the desired microstructure and properties.

The first results of increased osteoblast adhesion on the nanostructured metals were presented by WEBSTER and EJOFOR [2]. The grain boundaries favored the adhesion of the cells. A small degree of residual porosity after powder compaction has also played a role in the cell adhesion. It was proposed that an increased area of the surface defects exposed to the cell culture and to a larger degree of surface electron delocalization caused enhanced cell adhesion.

The main purpose of current research is to prevent failures caused by infection, by changing the biomaterial's properties and making them highly friendly for the surrounding tissues. In this work, the MA and powder technology processes were used to synthesize nanostructured Ti-45S5 bioglass-Ag composites. In order to test the toxicity of materials, as well as interaction between the tested materials, the *in vitro* cytocompatibility tests should be performed [11,27]. Recently, *in vitro* cytocompatibility tests of Ti-10% 45S5 bioglass nanocomposites have been conducted [11]. Fibroblasts play a key role in the initial stage of the implant integration with surrounding tissue. The study proved that no cytotoxic effects of the samples have been seen, both on the tested nanomaterial sample and microcrystalline titanium one. However, the cell growth intensity is strongly dependent on the surface structure of the material. The obtained results show that nanocrystalline Ti-45S5 bioglass sample displays good cytocompatibility compared with microcrystalline titanium. Survival rate of CCD-39Lu fibroblasts was higher in the presence of the nanocrystalline material as compared with microcrystalline material in the same concentration of the same interval. The proliferative activity of CCD-39Lu fibroblasts cultured in the presence of a nanocrystalline Ti-45S5 bioglass material correlates with viability of these cells in the culture and is dependent on the quantity of associated material.

In the present research, the activity of silver and 45S5 bioglass against the *S. mutans* and *S. aureus* was

evaluated. The Ti–bioglass–Ag composite showed the highest antibacterial activity against *S. aureus* and *S. mutans*. In both cases, the biofilm formation was reduced by more than 90% in comparison to microcrystalline titanium. According to the previous published research, when Ti–45S5 bioglass–Ag material can be immersed in body fluid, the metallic Ag particles on the surface of the Ti–45S5 bioglass–Ag could react with the body fluid and release ionized Ag into the surrounding fluid [28]. A steady and prolonged release of the silver biocide in a concentration level (0.1×10^{-9}) is capable of rendering antibacterial efficacy [28]. Silver particles had the highest antibacterial effect with minimal inhibition concentration (4.86 ± 2.71) $\mu\text{g/mL}$ and minimal bactericidal concentration $6.25 \mu\text{g/mL}$, respectively [29].

The mechanism for bacterial toxicity of tested Ti-based nanocomposites may include free metal ion toxicity arising from the dissolution of metals from the surface of the silver particles (e.g., Ag^+ from Ag) [30] or oxidative stress via the generation of reactive oxygen species (ROS) on crystal surfaces of some nanoparticles (e.g., silica (SiO_2), 45S5 bioglass) [31]. *S. mutans* in this study was killed not only by Ag particles, but also by SiO_2 particles. Silica has been found to inhibit bacteria adherence to oral biofilms [32]. The silica induces an unfavorable change in the biofilm, causing reduction of the adhesion, and therefore proliferation of bacteria.

The mechanism of action of silver particles on bacterial cells should be studied in details. Other mechanisms, which mainly include changes in bacterial cell wall permeability, removal of antimicrobial agents through efflux pumps of membrane, drug action site modification, antimicrobial agent's inactivation, etc., should be considered [18].

Recently, BESINIS et al [32] have investigated the toxicity of silver and silica nanoparticles (NPs) against *S. mutans*. The survival rate of bacteria under the effect of 100 mg/L Ag NPs in the media was 2% compared with 60% with chlorhexidine. Silica NPs had limited effects. Dialysis experiments showed negligible silver dissolution. Silver nanoparticles may extend their antibacterial application to methicillin-resistant *S. aureus* (MRSA) [33]. The antibacterial properties of silver nanoparticles against MRSA were investigated. Silver nanoparticles inhibited bacterial growth of both MRSA and non-MR *S. aureus*.

Evidence for the lack of toxicity of various bioglass formulations has been deduced from studies carried out, both *in vivo* and *in vitro*, in several different centers [34]. Titanium is not a poison metal and the human body can tolerate titanium in large dosis. Therefore, Ti-based composites containing bioglass and Ag have potential to be used in dentistry for infection control.

5 Conclusions

1) The Ti–45S5 bioglass–Ag nanocomposites were fabricated. The nanocomposites with about 8% porosity have average pore diameter of 3–9 μm , and the bulk Ti–bioglass–Ag exhibits reduced bacteria adhesion (*S. mutans* and *S. aureus*) in comparison with microcrystalline titanium.

2) Chemical composition and the implant microstructure are key factors for the success of implant adaptation. Therefore, the nanocrystalline Ti–45S5 bioglass–Ag composites may be an important step forward in the development of such a structure, which will support the process of osseointegration of the dental implant.

References

- [1] ALLAKER R P. The use of nanoparticles to control oral biofilm formation [J]. *J Dent Res*, 2010, 89: 1175–1186.
- [2] WEBSTER T J, EJOFOR J U. Increased osteoblast adhesion on nanophase metals: Ti, Ti6Al4V, and CoCrMo [J]. *Biomaterials*, 2004, 25: 4731–4739.
- [3] ZHANG L, WEBSTER T J. Nanotechnology and nanomaterials: Promises for improved tissue regeneration [J]. *Nano Today*, 2009, 4: 66–80.
- [4] XU W, HU W Y, LI M H, MA Q Q, HODGSON P D, WEN C E. Sol-gel derived HA/TiO₂ double coatings on Ti scaffolds for orthopaedic applications [J]. *Transactions of Nonferrous Metals Society of China*, 2006, 16(S1): s209–s216.
- [5] CHEN Liang-jian, LI Ting, LI Yi-min, HE Hao, HU You-hua. Porous titanium implants fabricated by metal injection molding [J]. *Transactions of Nonferrous Metals Society of China*, 2009, 19(5): 1174–1179.
- [6] PARK J W, KIM Y J, PARK C H, LEE D H, KO Y G, JANG J H, LEE C S. Enhanced osteoblast response to an equal channel angular pressing-processed pure titanium substrate with microrough surface topography [J]. *Acta Biomater*, 2009, 5: 3272–3280.
- [7] PYE A D, LOCKHART D E A, DAWSON M P, MURRAY A A, SMITH A J. A review of dental implants and infection [J]. *J Hospital Infection*, 2009, 72: 104–110.
- [8] MATUSIEWICZ H. Potential release of *in vivo* trace metals from metallic medical implants in the human body: From ions to nanoparticles—A systematic analytical review [J]. *Acta Biomater*, 2014, 10: 2379–2403.
- [9] XU Chun, ZHU Wen-feng. Comparison of microstructures and mechanical properties between forging and rolling processes for commercially pure titanium [J]. *Transactions of Nonferrous Metals Society of China*, 2012, 22(8): 1939–1946.
- [10] BOVAND D, YOUSEFPOUR M, RASOULI S, BAGHERIFARD S, BOVAND N, TAMAYOL A. Characterization of Ti–HA composite fabricated by mechanical alloying [J]. *Mater Design*, 2015, 65: 447–453.
- [11] KACZMAREK M, JURCZYK M U, RUBIS B, BANASZAK A, KOLECKA A, PASZEL A, JURCZYK K, MURIAS M, SIKORA J, JURCZYK M. *In vitro* biocompatibility of Ti–45S5 bioglass nanocomposites and their scaffolds [J]. *J Biomed Mater Res A*, 2014, 102: 1316–1324.
- [12] ZHANG Yuan-yuan, TAO Jie, PANG Ying-chun, WANG Wei, WANG Tao. Electrochemical deposition of hydroxyapatite coatings on titanium [J]. *Transactions of Nonferrous Metals Society of China*, 2006, 16(3): 633–637.
- [13] JURCZYK M U, JURCZYK K, NIESPODZIANA K,

- MIKLASZEWSKI A, JURCZYK M. Titanium–SiO₂ nanocomposites and their scaffolds for dental applications [J]. *Mater Charact*, 2013, 77: 99–108.
- [14] JURCZYK K, NIESPODZIANA K, JURCZYK M U, JURCZYK M. Synthesis and characterization of titanium–45S5 bioglass nanocomposites [J]. *Mater Design*, 2011, 32: 2554–2560.
- [15] ARIFIN A, SULONG A B, MUHAMAD N, SYARIF J, RAMLI M I. Powder injection molding of HA/Ti6Al4V composite using palm stearin as based binder for implant material [J]. *Mater Design*, 2015, 65: 1028–1034.
- [16] CAO W P, HENCH L. Bioactive materials [J]. *Ceramics Int*, 1996, 22: 493–507.
- [17] JURCZYK K, MIKLASZEWSKI A, NIESPODZIANA K, KUBICKA M, JURCZYK M U, JURCZYK M. Synthesis and properties of Ag-doped titanium–10wt.% 45S5 bioglass nanostructured scaffolds [J]. *Acta Metall Sin (Engl. Lett.)*, 2015, 28: 467–476.
- [18] JURCZYK M U, JURCZYK K, MIKLASZEWSKI A, JURCZYK M. Nanostructured titanium–45S5 bioglass scaffold composites for medical applications [J]. *Mater Design*, 2011, 32: 4882–4889.
- [19] RAI M K, DESHMUKH S D, INGLE A P, GADE A K. Silver nanoparticles: The powerful nanoweapon against multidrug-resistant bacteria—Review [J]. *J Appl Microbiology*, 2012, 112: 841–852.
- [20] RUAN H J, FAN C Y, ZHENG X B, ZHANG Y, CHEN Y K. *In vitro* antibacterial and osteogenic properties of plasma sprayed silver-containing hydroxyapatite coating [J]. *Chinese Sci Bull*, 2009, 54: 4438–4445.
- [21] CIOBANU C S, MASSUYEAU F, CONSTANTIN L V, PREDOI D. Structural and physical properties of antibacterial Ag-doped nano-hydroxyapatite synthesized at 100 °C [J]. *Nanoscale Res Lett*, 2011, 6: 613–621.
- [22] CHATZISTAVROU X, ZORBA T, KONTONASAKI E, CHRISSAFIS K, KOIDIS P, PARASKEVOPOULOS K M. Following bioactive glass behavior beyond melting temperature by thermal and optical methods [J]. *Phys Stat Sol*, 2004, 201: 944–951.
- [23] CLUPPER D C, HENCH L L. Highly bioactive P₂O₅–Na₂O–CaO–SiO₂ glass ceramics [J]. *J Non-Cryst Solids*, 2003, 318: 43–48.
- [24] RIZKALLA A S, JONES D W, CLARKE D B, HALL G C. Crystallization of experimental bioactive glass/ceramic systems [J]. *J Biomed Mater Res*, 1996, 32: 119–124.
- [25] MISHNAEVSKY L Jr, LEVASHOV R, VALIEV R Z, SEGURADO J, SABIROV I, ENIKEEV N, PROKOSHIN S, SOLOV'YOV A V, KOROTITSKIY A, GUTMANAS E, GOTMAN I, RABKIN E, PSAKH'E S, DLUHOŠ L, SEEFELDT M, SMOLIN A. Nanostructured titanium-based materials for medical implants: Modeling and development [J]. *Mater Sci Eng R: Reports*, 2014, 81: 1–19.
- [26] SURYANARAYNA C. Mechanical alloying and milling [J]. *Progr Mater Sci*, 2001, 46(1): 1–184.
- [27] CARLSSON L, RÖSTLUND T, ALBREKTSSON B, ALBREKTSSON T, BRÄNEMARK P I. Osseointegration of titanium implants [J]. *Acta Orthop Scand*, 1986, 57: 285–289.
- [28] KUMAR R, MÜNSTEDT H. Silver ion release from antimicrobial polyamide/silver composites [J]. *Biomaterials*, 2005, 26: 2081–2088.
- [29] HERNÁNDEZ-SIERRA J F, RUIZ F, PENA D C, MARTINEZ-GUTIÉRREZ F, MARTINEZ A E, GUILLÉN ADE J, TAPIA-PÉREZ H, CASTAÑÓN G M. The antimicrobial sensitivity of streptococcus mutans to nanoparticles of silver, zinc oxide, and gold [J]. *Nanomedicine*, 2008, 4: 237–240.
- [30] KIM J S, KUK E, YU K N, KIM J H, PARK S J, LEE H J, KIM S H, PARK Y K, PARK Y H, HWANG C Y, KIM Y K, LEE Y S, JEONG D H, CHO M H. Antimicrobial effects of silver nanoparticles [J]. *Nanomedicine*, 2007, 3: 95–101.
- [31] WONG M S, CHU W C, SUN D S, HUANG H S, CHEN J H, TSAI P J, LIN N T, YU M S, HSU S F, WANG S L, CHANG H H. Visible-light-induced bactericidal activity of a nitrogen-doped titanium photocatalyst against human pathogens [J]. *Appl Environ Microbiol*, 2006, 72: 6111–6116.
- [32] BESINIS A, de PERALTA T, HANDY R D. The antibacterial effects of silver, titanium dioxide and silica dioxide nanoparticles compared to the dental disinfectant chlorhexidine on *Streptococcus mutans* using a suite of bioassays [J]. *Nanotoxicology*, 2014, 8: 1–16.
- [33] AYALA-NÚÑEZ N V, VILLEGAS H H L, TURRENT L C I, PADILLA C R. Silver nanoparticles toxicity and bactericidal effect against methicillin-resistant *Staphylococcus aureus*: Nanoscale does matter [J]. *Nanobiotechnology*, 2009, 5: 2–9.
- [34] WILSON J, PIGOTT G H, SCHOEN F J, HENCH L L. Toxicology and biocompatibility of bioglasses [J]. *J Biomed Mater Res*, 1981, 15: 805–817.

纳米 Ti-45S5 生物玻璃–Ag 复合材料对变异链球菌和金黄色葡萄球菌的抗菌活性

K. JURCZYK¹, M. M. KUBICKA², M. RATAJCZAK², M. U. JURCZYK³, K. NIESPODZIANA⁴,
D. M. NOWAK², M. GAJECKA^{2,5}, M. JURCZYK⁴

1. Department of Conservative Dentistry and Periodontology, Poznan University of Medical Sciences, Bukowska 70, Poznan 60-812, Poland;

2. Faculty of Pharmacy, Department of Genetics and Pharmaceutical Microbiology, Poznan University of Medical Sciences, Swieczkiego 4, Poznan 60-781, Poland;

3. Division of Mother's and Child's Health, Poznan University of Medical Sciences, Polna 33, Poznan 60-535, Poland;

4. Institute of Materials Science and Engineering, Poznan University of Technology, Jana Pawla II 24, Poznan 61-138, Poland;

5. Institute of Human Genetics, Polish Academy of Sciences, Strzeszynska 32, Poznan 60-479, Poland

摘要: 利用机械合金化和在 1150 °C、氩保护气氛下退火 2 h 制备生物玻璃纳米复合材料。采用银对 Ti-45S5 生物玻璃进行化学改性。研究含银 Ti-10% 45S5 生物玻璃纳米复合材料对变异链球菌和金黄色葡萄球菌的抗菌活性。使用 XRD、SEM-EDS、TEM 对纳米复合材料的相组成、晶体结构和晶粒尺寸进行表征。体外细菌粘附研究表明，在纳米结构 Ti-45S5 生物玻璃表面的变异链球菌和金黄色葡萄球菌数量比微晶钛板表面的显著减少。钛基纳米结构生物材料将是下一代牙移植材料。

关键词: 45S5 生物玻璃；抗菌活性；银；钛；牙移植；变异链球菌；金黄色葡萄球菌